PROJECT REPORT

VALIDATION OF STRONG GROUND MOTION SIMULATIONS OF TWO HISTORICAL NEW ZEALAND SUBDUCTION ZONE EARTHQUAKES ON THE SCEC BROADBAND STRONG GROUND MOTION SIMULATION PLATFORM

Prepared for:

QuakeCoRE

January 27, 2017

AECOM

Jeff Bayless
Mehrdad Hosseini
Andreas Skarlatoudis
Paul Somerville

Table of Contents

Validation of Strong Ground Motion Simulations of two Historical New Zealand Subduction Zone Earthquakes on the SCEC Broadband Strong Ground Motion Simulation Platform

Introduction

In this project, we perform simulations of the ground motions from two historical New Zealand earthquakes using the Southern California Earthquake Center (SCEC) Broadband Strong Ground Motion Simulation Platform (BBP).

Our first case study is the 1931 Hawke's Bay earthquake. Hull (1990) concluded that this earthquake was a blind thrust fault in the accretionary prism of the subduction zone, not on the plate boundary itself. This earthquake was not recorded on strong motion instruments, but there is a detailed intensity map and we measure goodness of fit to the intensities by converting the results of our simulations to intensities. This earthquake is included because we consider that our modeled strong ground motion simulations may provide a useful basis for modeling the ground motions from large subduction earthquakes on the Hikurangi Trench. Secondly, we study the 15 July 2009 Mw 7.57 Fiordland earthquake. This earthquake occurred on the Puyesgur subduction zone at the southwestern end of the South Island (Beavan et al., 2010; Fry et al., 2010; Mahesh et al., 2011). The Mw 7.57 earthquake and a smaller earthquake (Mw 7.2) that occurred in 2003 were widely recorded on strong motion instruments.

In a related project, funded by SCEC, we have extended the BBP Graves and Pitarka (2015; GP2015 hereafter) hybrid simulation method to subduction events. Before this project, the BBP Graves & Pitarka method of combining low frequency synthetic seismograms and high frequency partly stochastic simulations had only been applied to shallow crustal earthquakes. In the past, at AECOM (formerly URS,) we have used a different hybrid method in which the long period simulations are done following GP2015, but the short period simulations were done using empirical source functions (Somerville et al., 1991; Somerville, 1993). In the BBP subduction implementation, we replace that method with the stochastic method used by GP2015. Using the SCEC BBP version of GP2015, we reproduced our previous validation of the procedure for the 2011 Tohoku earthquake. The validation shows little systematic bias in the prediction of the ground motions in the period range of 1 to 10 seconds. Further work is required to reduce the bias observed in the high frequency part (0.01 to 1s).

Hawke's Bay Earthquake Simulations

The historical 1931 Hawke's Bay earthquake, also known as the Napier earthquake, caused extensive damage and loss of life. Hull (1990) concluded that this earthquake was a blind thrust fault in the accretionary prism of the subduction zone, not on the plate boundary

itself. Nevertheless, we consider that our modeled strong ground motion simulations may provide a useful basis for modeling the ground motions from large subduction earthquakes on the Hikurangi Trench.

Seismic Velocity Model

We develop a generic 1D seismic velocity and density model for the Hawke's Bay region (Figure 1). This model is created by averaging profiles from the Eberhart-Phillips et al. (2010) model sampled within 100km of the fault plane, and modified in the upper 1.5 km to have a smooth transition to Vs30=863 m/s. For the long period component of the simulations, we calculate 1D Green's functions using this velocity model, and upload them to the SCEC BBP.
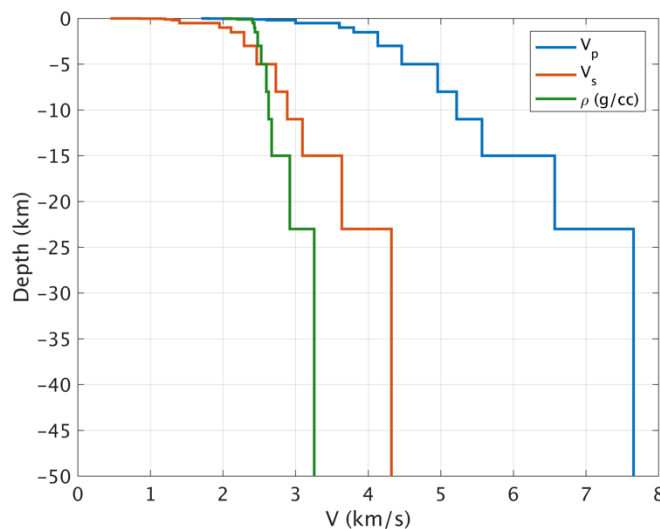

Figure 1. The 1D seismic velocity model used to represent the Hawke's Bay region.

Earthquake Source

Since the earthquake is determined by Hull (1990) to be imbricate reverse faulting in the accretionary prism of the Hikurangi subduction zone, we use a shallow crustal earthquake source model of the source. The fault trace length (80km), location, and orientation are as determined by Litchfield et al., 2013. The hypocenter location, moment magnitude (Mw 7.4) we use are from GeoNet (geonet.org.nz) with a focal depth of 20 km (Williams et al., 2013). The fault plane and hypocenter location are shown in Figure 2.

Ground Motion Intensities

Dowrick (1998) compiled MMI values covering most of the north island. These intensities are mapped in Figure 2 .
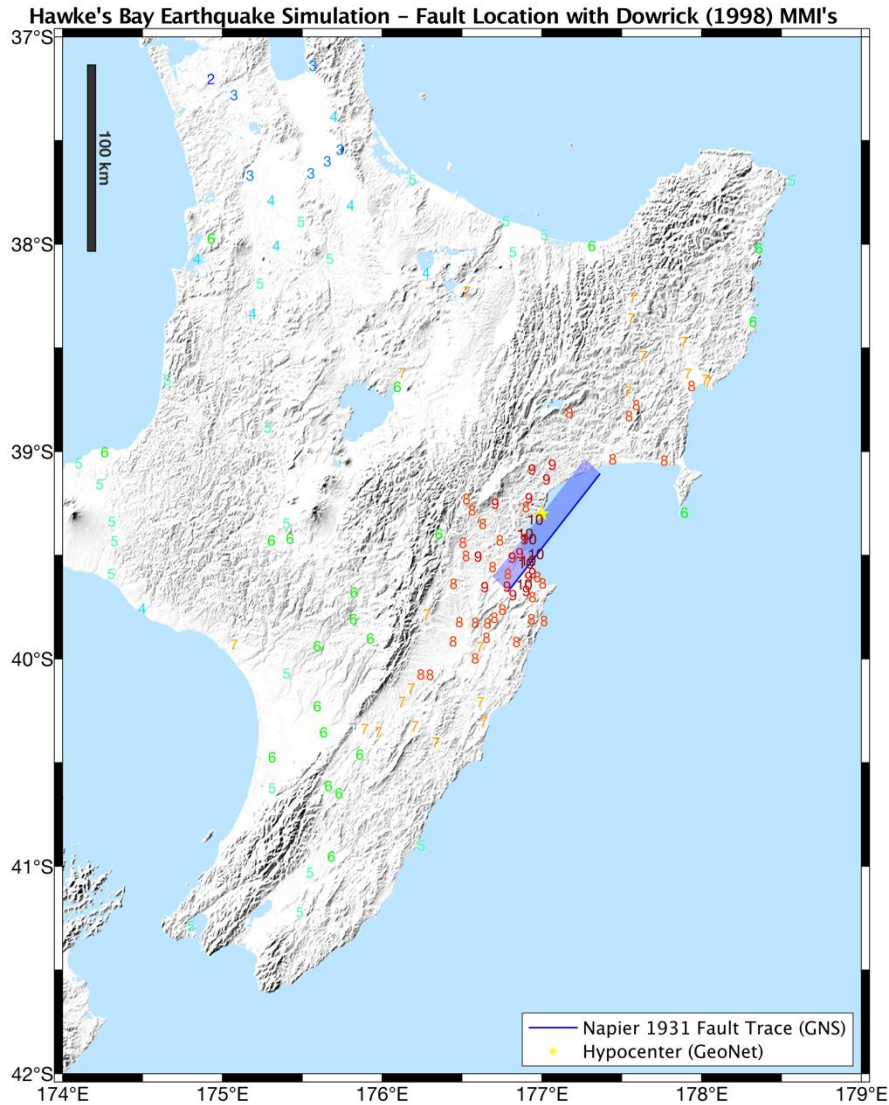
Figure 2. Region map of the north island, with the surface projection of the simulated fault plane in blue, hypocenter location marked by a gold star, and the Dowrick (1998) MMI values denoted on the map.

Simulation Results

We use the SCEC BBP version of GP2015 to create a source model using the parameters defined above (Figure 3), and perform simulations at each MMI location within Rjb distance of 100 km. We obtain three-component simulated acceleration time series at each site of interest. The strong motion simulations are adjusted for site effects using a Vs30-based empirical model applied to the Fourier amplitude spectra. Approximations for Vs30 at each site are obtained from topographic slope maps provided by the USGS (http://earthquake.usgs.gov/ hazards/apps/vs30/).

The simulations are converted to intensity using the ground motion intensity conversion equation (GMICE) of Caprio et al. (2015), which is based on the PGA, PGV and geographic

region. The spatial distribution of the MMI residuals (Figure 4) does not exhibit in general any significant trends. The converted intensity values from the simulations are in a good agreement with the MMI observations throughout the distance range examined and no strong trends with Vs30 are observed (Figure 5 through Figure 8).
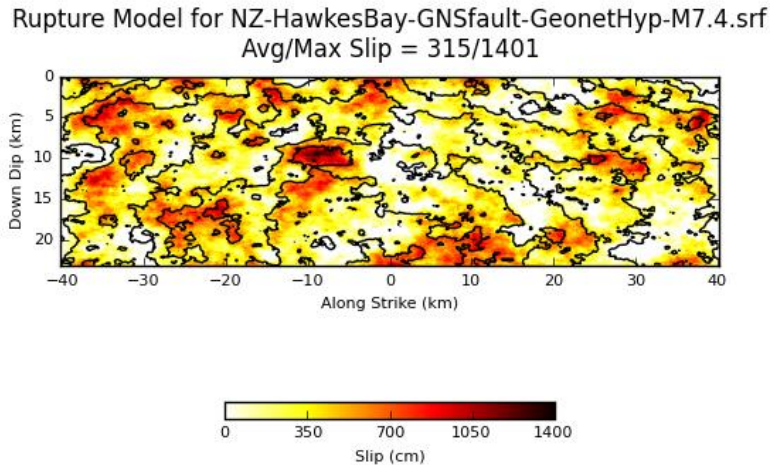

Figure 3. Illustration of the rupture model used for the Hawke's Bay simulation.
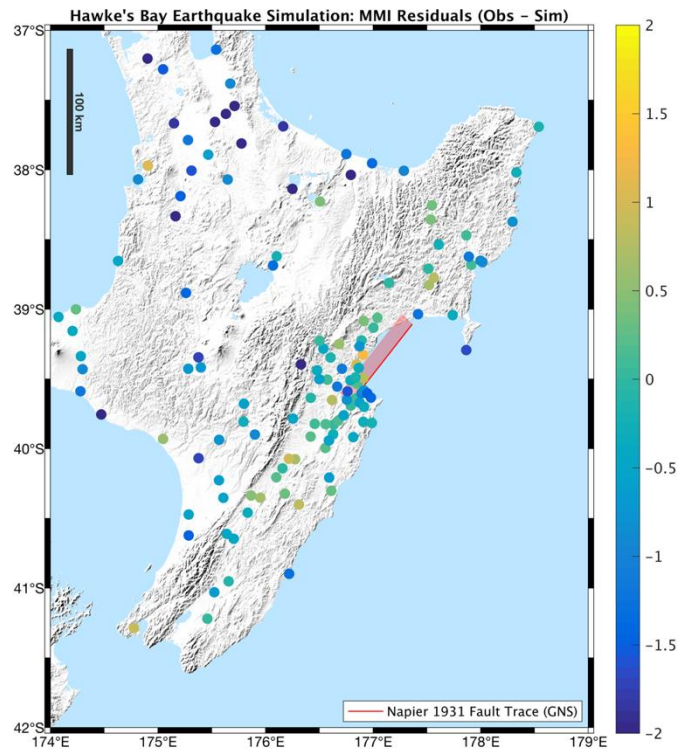

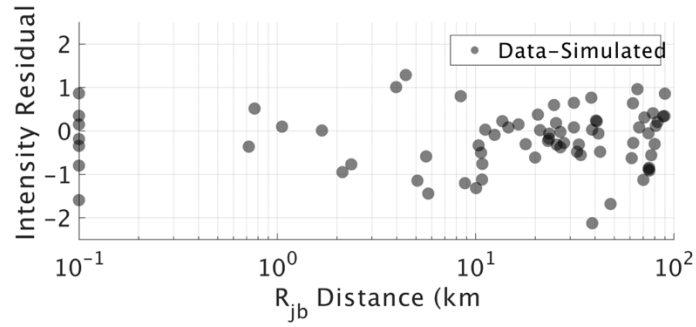**Figure 4.** Spatial distribution of simulation MMI residuals.

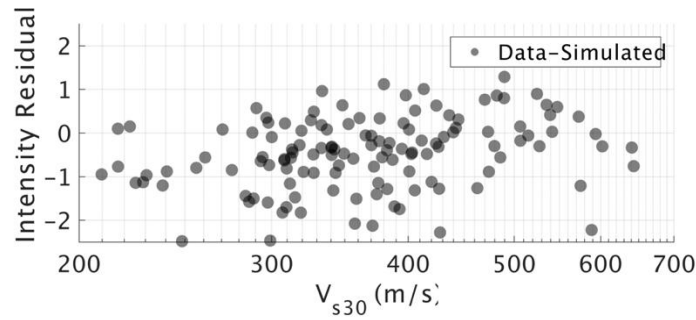**Figure 5.** MMI intensity residuals versus distance.

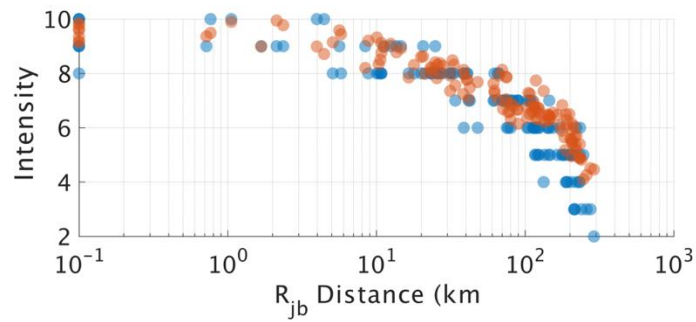**Figure 6.** MMI intensity residuals versus Vs30.

Figure 7. MMI versus distance. Dowrick (1998) values are in blue, and simulated values are in red.
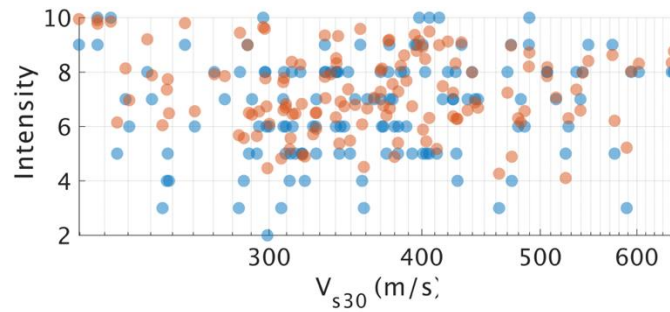

Figure 8. MMI versus Vs30. Dowrick (1998) values are in blue, and simulated values are in red.

Fiordland Earthquake Simulations

The 2009 Fiordland earthquake, also known as the Dusky Sound earthquake, occurred on the Puyesgur subduction zone at the southwestern end of the South Island (Beavan et al., 2010; Fry et al., 2010; Mahesh et al., 2011). This earthquake and a smaller earthquake (Mw 7.2) that occurred in 2003 were widely recorded on strong motion instruments. We use the SCEC BBP version of GP2015 to perform simulations of this subduction earthquake.

Seismic Velocity Model

We develop a generic 1D seismic velocity and density model for the Dusky Sound region of the south island (Figure 9). This model is created by averaging profiles from the Eberhart-Phillips et al. (2010) model sampled from the region with MMI VII in Fry et al., (2010). The s-wave velocities are modified in the upper 1.5 km to have a smooth transition to Vs30=863 m/s. For the long period component of the simulations, we calculate 1D Green's functions using this velocity model, and upload them to the SCEC BBP.
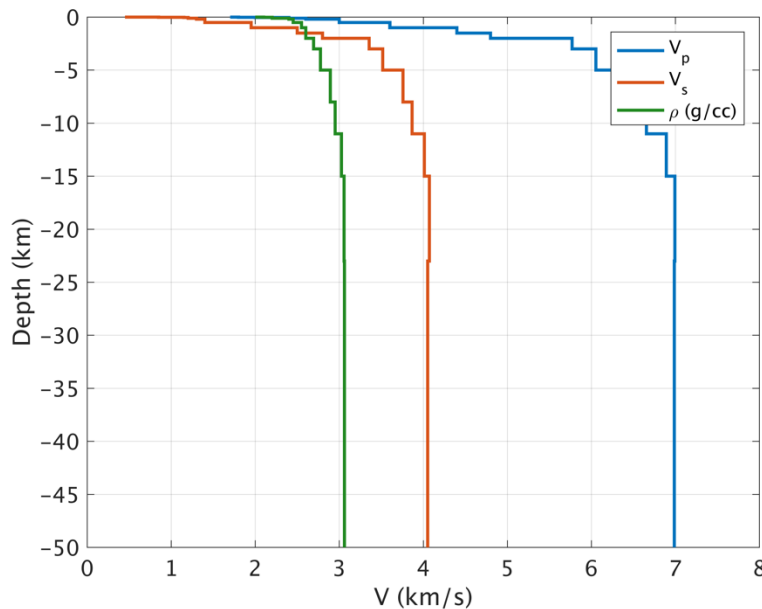

Figure 9. The 1D seismic velocity model used to represent the Dusky Sound region

Earthquake Source

Per GeoNet (geonet.org.nz), the earthquake rupture started at about 30 km depth and ruptured upwards and to the south, focusing energy offshore. Others (e.g. Fry et al., 2010; Gavin Hayes of USGS, personal communication) also report rupture propagating to the south with a strong slip asperity southwest of the hypocenter. We have selected the slip model from Gavin Hayes (USGS, personal communication) which has Mw 7.82, fault length 120 km, fault width 55 km, depth to the top of rupture 4.32 km, strike of 29 degrees, and dip of 26 degrees. Figure 10 shows the final slip distribution on the fault plane, and Figure 11 shows a map view of the surface projection of the fault.
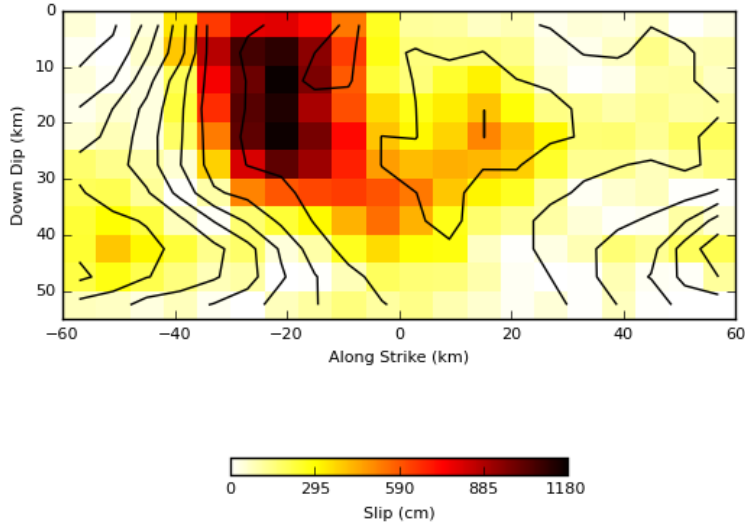
Figure 10. Illustration of the rupture model for the Fiordland simulation. The hypocenter is at approximately 20 km depth, to the northeast of the main slip asperity.

Simulation Stations

We select the nine stations south of latitude -44° and west of longitude 169°, where the strongest motions were recorded. These stations are identified in Figure 11, with the color scale denoting the recorded PGA.
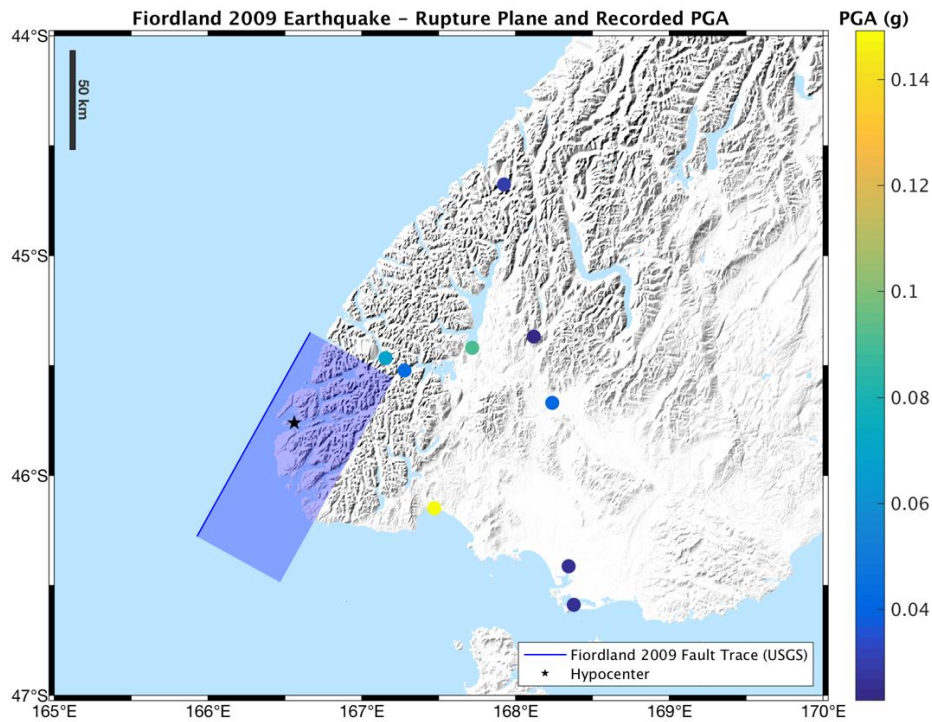

Figure 11. Map of the simulation region, with the surface projection of the simulated fault plane in blue, hypocenter location marked by the black star, and recording stations identified by colored circles. The color of each station is scaled to the recorded PGA.

A≡COM

9

Simulation Results

We use the SCEC BBP version of GP2015 to create a source model using the parameters defined above, and perform simulations at nine simulation stations. We obtain three-component simulated acceleration time series at each site. The strong motion simulations are adjusted for site effects using a Vs30-based empirical model applied to the Fourier amplitude spectra. Approximations for Vs30 at each site are obtained from topographic slope maps provided by the USGS (http://earthquake.usgs.gov/ hazards/apps/vs30/).

We calculate response spectra (5% damped, RotD50 component) of the simulated acceleration time series and the recorded time series. The results are summarized in a goodness-of-fit (GOF) plot, shown in Figure 12. In Figure 12, the red line is the mean natural log residual over the nine simulated stations, and the green bands represent plus and minus one standard deviation from the mean. The yellow band represents the 90% confidence interval on the mean. This figure shows that, outside the range of 1-3 seconds, our simulations are over-predicting the ground motions. For high frequencies (periods shorter than 1 second), the simulation method is based on the stochastic method, and there are parameters which need to be tuned. These parameters include the high-frequency stress parameter (set to 50 bars), the damping model, and diminution parameter kappa, among others. We would like to explore the effect of these parameters in future research, to tune them, and preferably create regionalized rules for GP2015.
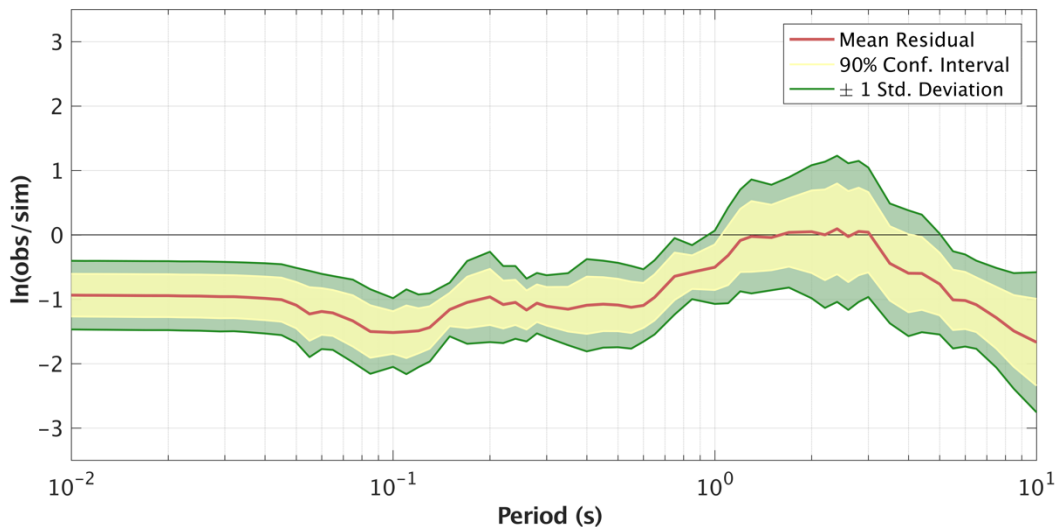

Figure 12. RotD50 component response spectra goodness-of-fit.

Figure 13 through Figure 16 show a comparison of the simulated and recorded RotD50 versus Rjb distance at four spectral periods. In Figure 17 the T=3.0s residuals are shown spatially; however, no trend with azimuth is observed.
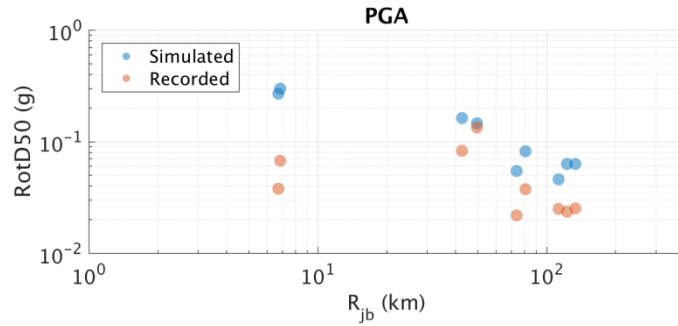
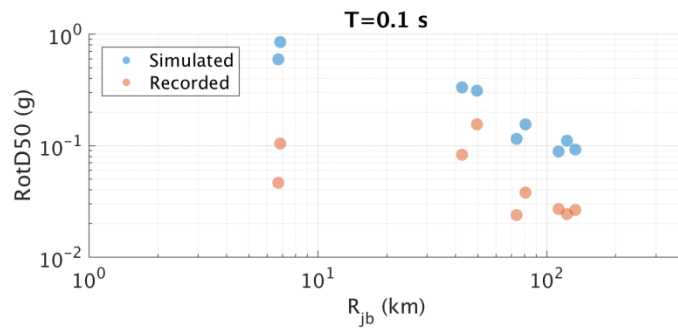**Figure 13.** Simulated (blue) and observed (red) PGA versus distance.

Figure 14. Simulated (blue) and observed (red) RotD50 at T=0.1s versus distance.
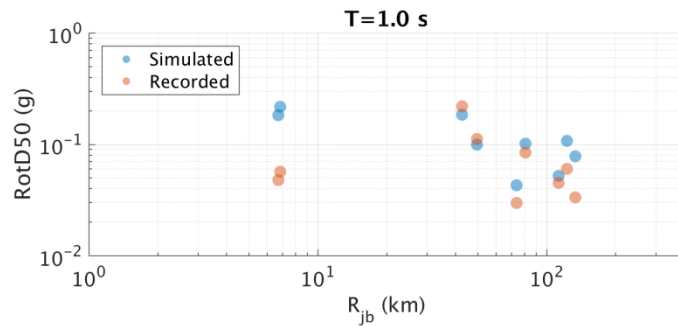

Figure 15. Simulated (blue) and observed (red) RotD50 at T=1.0s versus distance.
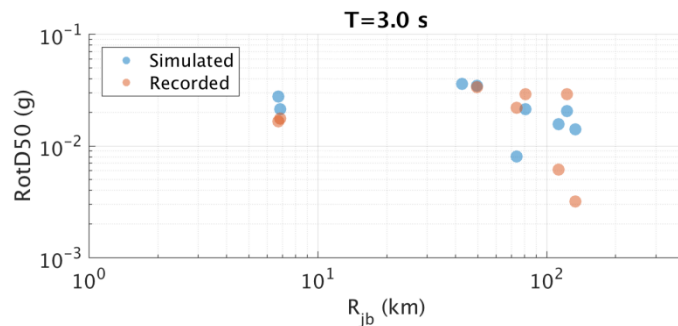

Figure 16. Simulated (blue) and observed (red) RotD50 at T=3.0s versus distance.
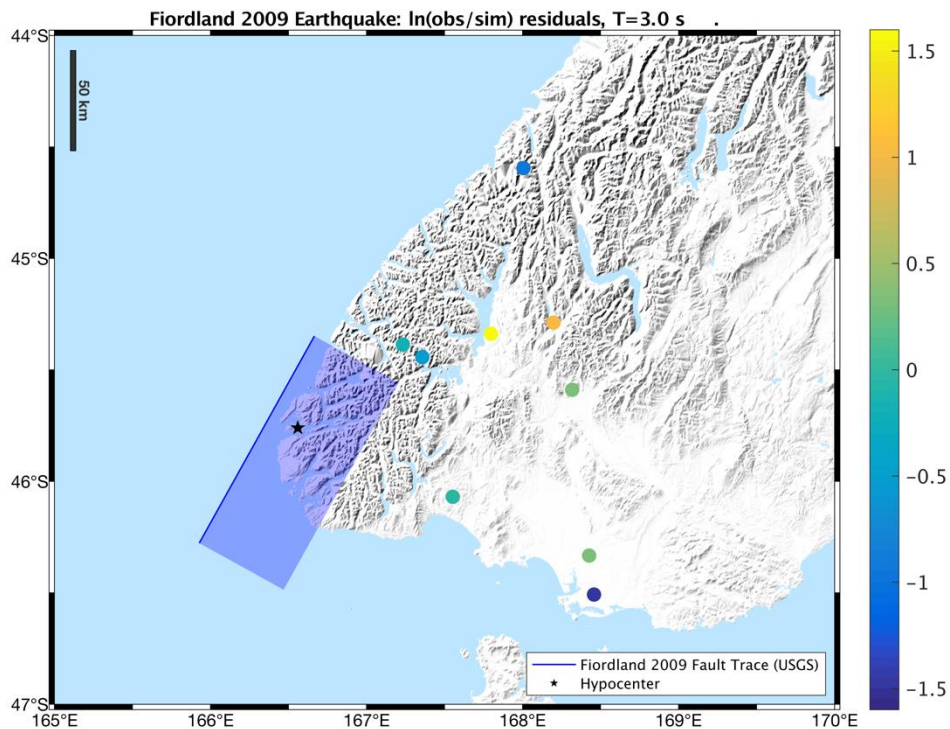
Figure 17. Map of the simulation region with color coded residuals for RotD50 at T=3.0s.

Conclusions

Using MMI as the intensity measure, the Hawke's Bay simulations produced comparable predictions to the records compiled by Dowrick (1998). We did not observe any strong bias or trends in the MMI residuals with distance or Vs30. Although this earthquake was not modeled as a subduction earthquake, we anticipate that our simulations may provide a useful basis for modeling the ground motions from large subduction earthquakes on the Hikurangi Trench in the future.

For the Fiordland simulation, we calculated response spectra from the simulated waveforms. We observe the same behavior from our previous validation of the 2011 Tohoku earthquake: that further work is required to reduce the RotD50 bias observed in the high frequency part (0.01 to 1s) of GP2015 for subduction earthquakes. In this case, we are simulating significantly larger ground motions than those which were recorded. In the future, we would like to study additional events, and perhaps more generalized source models for this same event, to tune the high frequency parameters and create regionalized rules for them. Simulating more events will also allow us to better evaluate the performance of the simulation method at low frequencies by having a larger sample size from which to draw conclusions.

References

Beavan, J., S. Samsonov, P. Denys, R. Sutherland, N. Palmer and M. Denham (2010). Oblique slip on the Puysegur subduction interface in the 2009 July MW 7.8 Dusky Sound earthquake from GPS and InSAR observations: implications for the tectonics of southwestern New Zealand. Geophys. J. Int. (2010) 183, 1265–1286.

Caprio, M., Bernadetta, T., Worden, B.C., Wiemer, S., and Wald, D.J. (2015). Ground Motion to Intensity Conversion Equations (GMICEs): A Global Relationship and Evaluation of Regional Dependency. Bulletin of the Seismological Society of America, 2015, Vol 105, 1476-1490.

Dowrick, D. (1998).   Damage and intensities if the magnitude 7.8 Hawkes Bay, New Zealand, earthquake. New Zealand Journal of Geology and Geophysics, 1998, Vol. 33., 139 – 163.

Eberhart-Phillips, D., Reyners, M., Bannister, S., Chadwick, M., Ellis, S. (2010). Establishing a Versatile 3-D Seismic Velocity Model for New Zealand. Seismological Research Letters Nov 2010, 81 (6) 992-1000; DOI: 10.1785/gssrl.81.6.992

Fry, B. et al. (2010). The Mw 7.6 Dusky Sound Earthquake 0f 2009: Preliminary Report. Bulletin of the New Zealand Society for Earthquake Engineering, Vol. 43, No. 1, March 2010.

Graves, R., and A. Pitarka (2015). Refinements to the Graves and Pitarka (2010) broadband ground motion simulation method, Seismol. Res. Lett. 86, no. 1, doi: 10.1785/0220140101.

Hayes G. (NEIC, New Zealand 2009). Preliminary Result of the July 15, 2009 Mw 7.6 Fiordland Earthquake

Hull, A.D. (1990). Tectonics of the 1931 Hawke's Bay earthquake. New Zealand Journal of Geology and Geophysics Volume 33, Issue 2, 309-320.

Litchfield, NJ, R Van Dissen, R Sutherland, PM Barnes, SC Cox, R Norris, RJ Beavan, R Langridge, P Villamor, K Berryman, M Stirling, A Nicol, S Nodder, G Lamarche, DJA Barrell, JR Pettinga, T Little, N Pondard, JJ Mountjoy, and K Clark. (2014) A model of active faulting in New Zealand. New Zealand Journal of Geology And Geophysics Vol. 57, Iss. 1,2014

Mahesh, P., B. Kunddu, P. Mahesh, J.K. Catherine, V.K. Gahalaut (2011). Anatomy of the 2009 Fiordland earthquake (Mw 7.8), South Island, New Zealand. Geoscience Frontiers, Volume 2, Issue 1, pages 17-22.

Somerville, P.G. (1993). Engineering applications of strong ground motion simulation, Tectonophysics, 218, 195-219.

Somerville, P.G., M.K. Sen and B.P. Cohee (1991). Simulation of strong ground motions recorded during the 1985 Michoacan, Mexico and Valparaiso, Chile earthquakes, Bull. Seism. Soc. Am., 81, 1-27.

Williams, C.A.; Eberhart-Phillips, D.; Bannister, S.C.; Barker, D.H.N.; Henrys, S.A.; Reyners, M.E.; Sutherland, R. 2013 Revised interface geometry for the Hikurangi subduction zone, New Zealand. Seismological Research Letters, 84(6): 1066-1073; doi: 10.1785/0220130035